

This article was downloaded by:

On: 26 January 2011

Access details: *Access Details: Free Access*

Publisher *Taylor & Francis*

Informa Ltd Registered in England and Wales Registered Number: 1072954 Registered office: Mortimer House, 37-41 Mortimer Street, London W1T 3JH, UK



Liquid Crystals

Publication details, including instructions for authors and subscription information:

<http://www.informaworld.com/smpp/title~content=t713926090>

Invited Lecture. Hexagonal cholesteric blue phases

R. M. Hornreich^a; S. Shtrikman^{ab}

^a Department of Electronics, Weizmann Institute of Science, Rehovot, Israel ^b Department of Physics, University of California, San Diego, La Jolla, California, U.S.A.

To cite this Article Hornreich, R. M. and Shtrikman, S.(1989) 'Invited Lecture. Hexagonal cholesteric blue phases', *Liquid Crystals*, 5: 3, 777 – 789

To link to this Article: DOI: 10.1080/02678298908026384

URL: <http://dx.doi.org/10.1080/02678298908026384>

PLEASE SCROLL DOWN FOR ARTICLE

Full terms and conditions of use: <http://www.informaworld.com/terms-and-conditions-of-access.pdf>

This article may be used for research, teaching and private study purposes. Any substantial or systematic reproduction, re-distribution, re-selling, loan or sub-licensing, systematic supply or distribution in any form to anyone is expressly forbidden.

The publisher does not give any warranty express or implied or make any representation that the contents will be complete or accurate or up to date. The accuracy of any instructions, formulae and drug doses should be independently verified with primary sources. The publisher shall not be liable for any loss, actions, claims, proceedings, demand or costs or damages whatsoever or howsoever caused arising directly or indirectly in connection with or arising out of the use of this material.

Invited Lecture

Hexagonal cholesteric blue phases

by R. M. HORNREICH and S. SHTRIKMAN†

Department of Electronics, Weizmann Institute of Science, 76100 Rehovot, Israel

Using Landau theory, the possibility that two and three dimensional hexagonal structures can exist in cholesteric liquid crystals with positive dielectric anisotropy in an applied electric or magnetic field is considered. Both are found to be thermodynamically stable in different regions of the chirality-temperature-field phase diagram, in agreement with reported experimental data. Further, the theoretical results indicate that two different three dimensional hexagonal phases, having the same space group (P6₃22) but different structure factors, may exist. Ways of verifying this prediction by optical and N.M.R. studies are considered. Also noted is the need to develop further the theoretical model to allow for the existence of the experimentally observed body-centred tetragonal structure.

1. Introduction

It is now well established that, in the absence of an external field, up to *three* thermodynamically stable phases can exist in a narrow temperature range between the disordered and usual helicoidal structures in cholesteric liquid crystal systems [1, 2]. Known collectively as cholesteric blue phases (BP), these intermediate phases have been studied extensively both experimentally and theoretically over the past decade and their properties are, in the main, well understood. For example, there is a wide range of data and model calculations [1, 2] indicating that two of these phases have cubic structures (BPI, body-centred; BPII, simple cubic). The third, BPIII (also known as the fog or grey phase), is also non-birefringent but, although several possibilities have been considered [3, 4], its structure remains one of the outstanding puzzles in the physics of liquid crystals.

When an electric or magnetic field is applied, Hornreich *et al.* [5] pointed out that a new phase, having a hexagonal structure, could appear. This prediction was based upon a comparison of the free energies of the cubic BP, the helicoidal cholesteric C phase, and a simple two dimensional hexagonal one (H^{2D}). Although for physical values of the cholesteric pitch, H^{2D} is never thermodynamically stable in the absence of an external field, it can become so when a field is applied. This is possible as, in the weak field limit, the order parameter couples to the *square* of the field strength for C and H^{2D} whereas, for cubic phases, the coupling is to the *fourth power* of the field [5, 6]. Experimental work [7] confirmed this theoretical prediction, there is indeed a region in the phase diagram in which H^{2D} is the thermodynamically stable phase. However, this was *not* the only non-cubic structure found. At least three non-cubic BP have been

† Also with the Department of Physics, University of California, San Diego, La Jolla, California 92093, U.S.A.

observed, two with hexagonal and one with tetragonal symmetry [7, 8]. There is therefore the question as to whether the Landau theory of BP [2], which successfully explained (with *no* free parameters) the existence of the cubic phases BPI and BPII which appear in the absence of an external field, can also describe the extended phase diagram found experimentally when a field is applied.

We give here a partial answer to this question by extending, in the following section, the field-dependent Landau model considered earlier [5] so as to include three dimensional hexagonal (H^{3D}) structures as well as H^{2D} . The model calculations are compared with the available data, and possible avenues for additional experimental studies are indicated. Further extensions of the model are discussed in the final section, where we also summarize our findings.

2. Field-induced hexagonal phases

2.1. The Landau free energy

A convenient form for the Landau free energy functional for the case of cholesteric (chiral) systems in the presence of an external field has been given elsewhere. [2b, 5, 6]. We give, therefore, only a brief summary here. Landau theory is based upon a symmetric traceless tensor order parameter which, for the case of an applied *electric* field, may be taken as

$$\varepsilon_{ij}(\mathbf{r}) \equiv e_{ij}^d(\mathbf{r}) - \frac{1}{3}\text{Tr}(e^d)\delta_{ij}, \quad (1)$$

where e_{ij}^d is the dielectric tensor. The free energy functional, to fourth order in ε_{ij} itself and to second order in ε_{ij} and its spatial derivatives, is given by [9]

$$F_c = V^{-1} \int d\mathbf{r} \left[\frac{1}{2}(a\varepsilon_{ij}^2 - 2de_{ijl}\varepsilon_{im}\varepsilon_{jn,l} + c_1 e_{ij,l}^2 + c_2 e_{ij,l}^2) - \beta\varepsilon_{ij}\varepsilon_{jl}\varepsilon_{ii} + \gamma(e_{ij}^2)^2 - (1/8\pi)\varepsilon_{ij}E_iE_j \right]. \quad (2)$$

Here a is proportional to a reduced temperature, d , β , γ , c_1 and c_2 are temperature-independent parameters, V is volume, e_{ijl} is the usual antisymmetric third order tensor, $\varepsilon_{ij,l} \equiv \partial\varepsilon_{ij}/\partial r_l$, \mathbf{E} is an applied electric field, and we sum on all repeated indices. For thermodynamic stability (i.e. the requirement [2, 10, 11] that F_c be positive for sufficiently large values of the order parameter and its derivatives), the quantities γ , c_1 and $c_1 + \frac{2}{3}c_2$ must all be positive. We use the reduced quantities [2b, 5, 10, 11]

$$\left. \begin{aligned} \mu_{ij} &= \varepsilon_{ij}/(\beta/\sqrt{6\gamma}), & f &= F_c/(\beta^4/36\gamma^3), & \frac{1}{4}t &= (3\gamma/\beta^2)a, \\ \frac{1}{4}\xi_R^2 &= (3\gamma/\beta^2)c_1, & c_2/c_1 &= \varrho, & \kappa &= (d/c_1)\xi_R = q_C\xi_R, \\ \mathbf{x} &= \mathbf{r}/\xi_R, & \mu_{ij,l} &= \mu_{ij}/\partial x_l, & v &= V/\xi_R^3, & \mathbf{e} &= \mathbf{E}/(4\pi\beta^3/3\gamma^2)^{1/2}. \end{aligned} \right\} \quad (3)$$

Equation (2) then becomes

$$f = v^{-1} \int d\mathbf{x} \left[\frac{1}{4}(t\mu_{ij}^2 - 2\kappa e_{ijl}\mu_{im}\mu_{jn,l} + \mu_{ij,l}^2 + \varrho\mu_{ij,l}^2) - \sqrt{6}\mu_{ij}\mu_{jl}\mu_{ii} + (\mu_{ij}^2)^2 - \sqrt{6}\mu_{ij}e_i e_j \right]. \quad (4)$$

Note particularly that the pitch-temperature-field or (κ, t, \mathbf{e}) phase diagram obtained by minimizing f can depend, at most, only upon a single parameter, ϱ . Equation (4) can also be obtained for the case of an applied magnetic field \mathbf{H} by making the

following replacements in equations (1)–(3):

$$\left. \begin{aligned} \chi_{ij} &\leftrightarrow \epsilon_{ij}, \\ (2V)^{-1} \int d\mathbf{r} \chi_{ij} H_i H_j &\leftrightarrow (8\pi V)^{-1} \int d\mathbf{r} \epsilon_{ij} E_i E_j, \\ \mathbf{H}/(\beta^3/3\gamma^2)^{1/2} &\leftrightarrow \mathbf{E}/(4\pi\beta^3/3\gamma^2)^{1/2}. \end{aligned} \right\} \quad (5)$$

As we are interested in periodic structures, we naturally expand $\mu_{ij}(\mathbf{x})$ in Fourier components [2, 10, 11]:

$$\mu_{ij}(\mathbf{x}) = \sum_{\sigma, n} N^{-1/2}(\sigma) \mu_{ij}(\sigma, n) \exp(i\mathbf{q}_{\sigma, n} \cdot \mathbf{x}). \quad (6)$$

In equation (6), $n = -N(\sigma)/2, \dots, -1, 1, \dots, N(\sigma)/2$ runs over the set of $N(\sigma)$ wavevectors of magnitude $q_\sigma = |\mathbf{q}_{\sigma, n}| = \sigma^{1/2}q$ with $\mathbf{q}_{\sigma, -n} = -\mathbf{q}_{\sigma, n}$. The parameter σ (not necessarily integer) indexes wavevectors of different magnitudes. If $\mu_{ij}(\mathbf{x})$ includes a $q = 0$ term, it is labelled by $\sigma = n = 0$. The wavevector parameter q is dimensionless (i.e. it is in units of ξ_R^{-1}) and is fixed by minimizing the free energy. In addition, for hexagonal structures, one ratio of parameters σ is also fixed via energy minimization. The fixing of these two parameters determines the size and shape, respectively, of the hexagonal unit cell.

The tensors $[\mu_{ij}(\sigma, n)]$ can each be expanded in terms of five basis tensors as follows:

$$\begin{aligned} [\mu_{ij}(\sigma, n)] &= \sum_{m=-2}^2 \mu_m(\sigma) e^{i\psi_m(\sigma, n)} [M_m(\sigma, n)] \\ &= \frac{1}{2} \left[\mu_2 e^{i\psi_2} \begin{pmatrix} 1 & i & 0 \\ i & -1 & 0 \\ 0 & 0 & 0 \end{pmatrix} + \mu_1 e^{i\psi_1} \begin{pmatrix} 0 & 0 & 1 \\ 0 & 0 & i \\ 1 & i & 0 \end{pmatrix} + \sqrt{\frac{2}{3}} \mu_0 e^{i\psi_0} \begin{pmatrix} -1 & 0 & 0 \\ 0 & -1 & 0 \\ 0 & 0 & 2 \end{pmatrix} \right. \\ &\quad \left. + \mu_{-1} e^{i\psi_{-1}} \begin{pmatrix} 0 & 0 & -1 \\ 0 & 0 & i \\ -1 & i & 0 \end{pmatrix} + \mu_{-2} e^{i\psi_{-2}} \begin{pmatrix} 1 & -i & 0 \\ -i & -1 & 0 \\ 0 & 0 & 0 \end{pmatrix} \right]. \end{aligned} \quad (7)$$

Here $\mu_m(\sigma) \geq 0$ and we have suppressed the indices (σ, n) on μ_m and ψ_m in the final expression. The basis tensors are defined in a local right-handed coordinate system $(\hat{\xi}, \hat{\eta}, \hat{\zeta})$ for each (σ, n) with the polar axis $\hat{\zeta} \equiv \hat{q}_{\sigma, n}$. The directions of the other two axes are reflected in the choice of phases $\psi_m(\sigma, n)$. Requiring that $\hat{\xi}(\sigma, n) = \hat{\xi}(\sigma, -n)$ and $\hat{\eta}(\sigma, n) = -\hat{\eta}(\sigma, -n)$ results in $\psi_m(\sigma, n) = -\psi_m(\sigma, -n)$. This prescription determines the $(\sigma, -n)$ term conjugate to each $(\sigma, n > 0)$ one; it thus suffices to specify the latter.

Using equations (6) and (7), the calculation of the quadratic part f_2 of f is straightforward. The result is [2b, 10, 11]

$$f_2 = \frac{1}{4} \sum_{\sigma, m} \{t - \kappa m q \sigma^{1/2} + [1 + \frac{1}{6} \varrho(4 - m^2) q^2 \sigma] \mu_m^2(\sigma)\}. \quad (8)$$

Since, in Landau theory, the explicit q -dependence of f appears only in f_2 , we have $\partial f / \partial q = \partial f_2 / \partial q = 0$ and

$$q = \frac{1}{2} \kappa \left\{ \sum_{\sigma, m} [m \sigma^{1/2} \mu_m^2(\sigma)] \right\} / \left\{ \sum_{\sigma, m} [1 + \frac{1}{6} \varrho(4 - m^2) \sigma \mu_m^2(\sigma)] \right\}. \quad (9)$$

In some applications, a more convenient quantity is [10, 11]

$$r \equiv \sqrt{2} q/\kappa = (q\zeta_R^{-1})/(q_C/\sqrt{2}). \quad (10)$$

Of course, any $\sigma = 0$ term in equation (8) is excluded from the sums in equation (9).

To summarize, the scaled average Landau free energy density of cholesterics has the form

$$f = \frac{1}{4} \sum_{\sigma, m} \{t - \kappa m q \sigma^{1/2} + [1 + \frac{1}{8} \rho(4 - m^2)] q^2 \sigma\} \mu_m^2(\sigma) + v^{-1} \int d\mathbf{x} [-\sqrt{6} \mu_{ij} \mu_{jl} \mu_{li} + (\mu_{ij}^2)^2 - \sqrt{6} \mu_{ij} e_i e_j], \quad (11)$$

with q determined via equation (9). Our objective is to minimize the free energy functional $f([\mu])$ at an arbitrary point in the (κ, t, \mathbf{e}) -space. As noted earlier, there is only a single parameter (ρ) in the scaled free energy expression.

The primary ingredient of all ordered cholesteric phases can be understood by considering the lowest order (quadratic) part of the free energy. For $\kappa \neq 0$ the system is chiral and the minimum of f_2 is necessarily at $q \neq 0$. The thermodynamic stability requirement, $1 + \frac{2}{3} \rho > 0$, guarantees that the ground state of f_2 lies on the $m = 2$ branch of the spectrum. This branch is, in fact, the lowest lying for *all* σ provided that $\rho > 0$, a condition satisfied [9] by most liquid crystals near the order-disorder thermodynamic phase boundary. It follows that transverse $m = 2$ Fourier components are an essential part of the structure factor of all ordered cholesteric phases. As was done [2, 10, 11] for the cubic BP, we shall restrict the order parameter to have only $m = 2$ Fourier components for all $\sigma \neq 0$. In addition, we allow an $m = 0$, $\sigma = 0$ component in non-cubic structures [2, 5, 10]. Indeed, it is only this term in the Fourier series which couples to the applied field. Then all terms in f proportional to q vanish and the (κ, t, \mathbf{e}) phase diagram is *parameter-independent*.

2.2. Hexagonal structures

The $\mathbf{e} = \mathbf{0}$ free energy of a planar hexagonal phase was calculated originally by Brazovskii and Dmitriev [12]. Their model was based upon a single equilateral triangle of wavevectors (with $n > 0$), which we label $\sigma = \sigma_b$. These wavevectors are of magnitude $q_b = \sigma_b^{1/2} q$ and their respective local axis systems are summarized in table 1. It is straightforward to show [2b, 10] that the energy of this structure is

Table 1. Wavevectors and associated principal axis systems ($\hat{\xi}, \hat{\eta}, \hat{\zeta}$) in the Fourier decomposition of the order parameter $\mu_{ij}(\mathbf{x})$. Here $\mathbf{q}_{bn} \equiv \mathbf{q}_{\sigma_b, n}$, etc.

Wavevectors ($\hat{\zeta} = \hat{q}$)	$\hat{\xi}$	$\hat{\eta}$
$q_{b1} = cq(-\hat{x} + \hat{y})/\sqrt{2}$	$(\hat{x} + \hat{y} + \hat{z})/\sqrt{3}$	$(\hat{x} + \hat{y} - 2\hat{z})/\sqrt{6}$
$q_{b2} = cq(-\hat{y} + \hat{z})/\sqrt{2}$	$(\hat{x} + \hat{y} + \hat{z})/\sqrt{3}$	$(\hat{y} + \hat{z} - 2\hat{x})/\sqrt{6}$
$q_{b3} = cq(-\hat{z} + \hat{x})/\sqrt{2}$	$(\hat{x} + \hat{y} + \hat{z})/\sqrt{3}$	$(\hat{z} + \hat{x} - 2\hat{y})/\sqrt{6}$
$q_h = sq(\hat{x} + \hat{y} + \hat{z})/\sqrt{3}$	$(\hat{x} + \hat{y} - 2\hat{z})/\sqrt{6}$	$(-\hat{x} + \hat{y})/\sqrt{2}$
$q_{dn} = -q_{bn} + q_h$	$\hat{\xi}_{dn} = \hat{\eta}_{dn} \times \hat{q}_{dn}$	$\hat{\eta}_{dn} = -\hat{\eta}_{bn} \quad (n = 1, 2, 3)$
$q_{d(n+3)} = q_{bn} + q_h$	$\hat{\xi}_{d(n+3)} = \hat{\eta}_{d(n+3)} \times \hat{q}_{d(n+3)}$	$\hat{\eta}_{d(n+3)} = \hat{\eta}_{bn} \quad (n = 1, 2, 3)$

Nematic-like component: $[M_0] = [3\zeta_i \zeta_j - \delta_{ij}]/\sqrt{6}$ with $\hat{\zeta} = (\hat{x} + \hat{y} + \hat{z})/\sqrt{3}$ and $i = x, y, z$.

minimized by setting all $\psi_2(\sigma_b, n) = 0$. This structure, however, is never thermodynamically stable at physically relevant values of the chirality parameter κ [10, 13]. (This changes in the $\kappa \rightarrow \infty$ limit [14].) Even a more realistic planar model, in which an $m = \sigma = 0$ nematic-like (n) component (oriented normal to the plane of the $\mathbf{q}_{\sigma_b, n}$ wavevectors, see table 1) is included in the order parameter $\mu_{ij}(\mathbf{x})$, does not become the ground state at physical values of κ in the absence of an applied field [10, 13]. This latter structure (space group $p6$; henceforth referred to as H^{2D}) can, however, become thermodynamically stable when $\mathbf{e} \neq \mathbf{0}$. This theoretical prediction [5] has since been confirmed experimentally [7]. Moreover, there is an *additional* thermodynamically stable hexagonal structure in the (κ, t, \mathbf{e}) phase diagram in addition to H^{2D} , having a three rather than a two dimensional character [7]. We now turn to its theoretical description.

To model a three dimensional hexagonal structure, at least one additional $\sigma \neq 0$ Fourier component in $\mu_{ij}(\mathbf{x})$ is required. It's associated wavevector is perpendicular to the basal (b) plane (i.e. to the plane formed by the equilateral triangle of wavevectors $\mathbf{q}_{\sigma_b, n}$). We label this wavevector $\mathbf{q}_{\sigma_h, n}$, with magnitude $q_h = \sigma_h^{1/2} q$. The subscript indicates that this vector is along the hexagonal (h) axis of the cell. Of course, $n = 1$ for this set of wavevectors; we therefore drop this index. The local axis system associated with \mathbf{q}_{σ_h} is given in table 1. As discussed earlier, we take its tensor amplitude to have an $m = 2$ component only. Since $\mathbf{q}_{\sigma_h} \perp \mathbf{q}_{\sigma_b, n}$, adding this Fourier component alone does not result in any new contributions to the third order term f_3 in the Landau free energy. Such contributions, which are essential if the structure is to become the ground state somewhere in the phase diagram, come only from *triangles* of wavevectors [2b, 10]. We must therefore add at least one further set of wavevectors which, taken together with those in the basal plane and that along the hexagonal axis, form triangles. This set of diagonal (d) wavevectors are just the sums: $\pm \mathbf{q}_{\sigma_b, n} + \mathbf{q}_{\sigma_h}$ and their negatives. There are then *six* $n > 0$ vectors in this set, which we label $\mathbf{q}_{\sigma_d, n=1, \dots, 6}$. Their magnitude is $q_d = \sigma_d^{1/2} q$, with $\sigma_d = \sigma_b + \sigma_h$, and their local axis systems are given in table 1. As always, they have tensor amplitudes with an $m = 2$ component only. A diagram of the wavevectors with $\sigma = \sigma_b, \sigma_h$ and σ_d is given in figure 1.

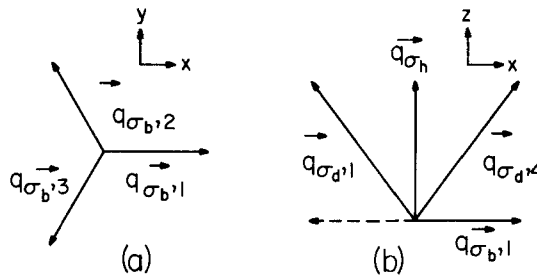


Figure 1. Wavevectors in the Fourier decomposition of the order parameter for H^{3D} . Shown are (a) the three basal plane wavevectors, and (b) the x - z plane cross section, containing the vectors $\pm \mathbf{q}_{\sigma_b, 1}$, \mathbf{q}_{σ_h} , $\mathbf{q}_{\sigma_d, 1}$ and $\mathbf{q}_{\sigma_d, 4}$. The other σ_d wavevectors are obtained by $2\pi/3$ rotations about z . Details are given in table 1.

Consider now the phases $\psi_2(\sigma, n)$ for the three dimensional structure. For any hexagonal symmetry class, the three $n > 0$ basal plane wavevectors in table 1 must have the same phase, thus $\psi_2(\sigma_b, n = 1, 2, 3) = \psi_b$. As noted by Piéranski, Cladis and Barbet-Massin [7], the possible space groups for a hexagonal BP are $P6_1 22 (D_6^2)$ and $P6_2 22 (D_6^4)$. In both of these, the basal plane wavevectors $\mathbf{q}_{\sigma_b, n}$ are twofold

symmetry axes of the space group; thus $\psi_b = 0$ or π . In addition, it is clear that the free energy of the structure cannot depend upon $\psi_2(\sigma_h)$, which we therefore set equal to zero.

Consider next the phases $\psi_2(\sigma_d, n = 1, \dots, 6)$. These *do* depend upon which of the previous space groups characterizes the hexagonal phase. For P6₁22 three successive applications of the 6₁ screw element take $\mathbf{q}_{\sigma_d,1}$ to $\mathbf{q}_{\sigma_d,4}$. There is also an overall translation of half of a unit cell along the hexagonal axis, equivalent to a phase shift of π . Now, since the wavevectors $\pm \mathbf{q}_{\sigma_b,1}$ have the *same* associated phase, it follows that the contributions to f_3 from the two triangles, $(\mathbf{q}_{\sigma_b,1}, -\mathbf{q}_{\sigma_b,1}, \mathbf{q}_{\sigma_d,1})$ and $(-\mathbf{q}_{\sigma_b,1}, -\mathbf{q}_{\sigma_b,1}, \mathbf{q}_{\sigma_d,4})$, have *opposite algebraic signs*. Thus, the net contribution from all triangles of this type to f_3 *vanishes* for the space group P6₁22. On the other hand, for P6₂22, the total phase shift resulting from three successive applications of the 6₂ screw element is 2π . In this case, the contributions to f_3 from the two triangles noted previously have the *same* algebraic sign. Thus the net contribution from all the triangles of this type of f_3 need *not* vanish and it can result [2b] in a lowering of the free energy of an P6₂22 structure. We therefore concentrate on this space group as an H^{3D} model structure.

From figure 1, we see that successive 6₂ rotations about the hexagonal axis permute the $\mathbf{q}_{\sigma_d,n}$ wavevectors in the order: 1 → 6 → 2 → 4 → 3 → 5 → 1, etc. In addition, each such operation shifts the phase of the complex Fourier amplitude associated with each $\mathbf{q}_{\sigma_d,n}$ wavevector by $2\pi/3$. Thus, in order for each triangle composed of a base, hexagonal and diagonal wavevector to contribute *equally* to f_3 , it is necessary to balance this phase shift by setting

$$\psi_2(\sigma_d, n + 1) = \psi_2(\sigma_d, n) - 2\pi/3, \quad (12)$$

for $n = 1, \dots, 5$. Finally, in order to *maximize* (the magnitude of) this third order contribution, we set [2b] $\psi_2(\sigma_d, 1) = 0$ or π .

To summarize, we model possible H^{3D} phases by an order parameter which is invariant under the space group P6₂22. It contains four independent amplitudes: $\mu_2(\sigma_b) \equiv \mu_b, \mu_2(\sigma_h) \equiv \mu_h, \mu_2(\sigma_d) \equiv \mu_d$ and $\mu_0(\sigma_n = 0) \equiv \mu_n$. These are, respectively, the $m = 2$ Fourier amplitudes associated with the basal, hexagonal and diagonal wavevectors, and that of the zero wavevector (nematic-like) tensor component which couples to the applied field. We consider here only the case $\mu_n > 0$ (positive electric and/or magnetic anisotropy). Since, without loss of generality, we can set $\sigma_d = 1$, there are only two other independent quantities, the dimensional scale q and the ratio σ_b/σ_d . We next calculate the free energy f as a function of $\mu_j(\mathbf{x})$, i.e. as a function of these six scalar quantities. These are then fixed by minimization of the free energy.

For cubic and icosahedral BP structures, we have shown [2b, 11, 15] that the coefficients of the third and fourth order terms making up the relevant free energy expression can be efficiently obtained numerically. That is, each such term is a product of a coefficient and three or four of the Fourier amplitudes; these coefficients are easily obtained with six figure accuracy by numerical integration. For H^{3D}, however, the coefficients are, in general, dependent upon σ_b/σ_h . We have therefore employed a different approach, wherein REDUCE, a symbolic manipulator, was used to calculate free energy terms. For this purpose, the applied field \mathbf{e} was taken to be along the hexagonal axis of the structure since this minimizes $f_{\text{H}^{3\text{D}}}$ for $\mu_n > 0$. In addition, the phases $\psi_2(\sigma_b, n)$ and $\psi_2(\sigma_d, 1)$ were set equal to zero. This is not a serious restriction, as the free energy functional corresponding to values of π for either or both of these

phase factors can be obtained by simply reversing the algebraic sign of terms containing odd powers of μ_b and/or μ_d in the expression for the free energy.

The resulting expression for the H^{3D} free energy $f_{H^{3D}}$ is

$$f_{H^{3D}} = f_1 + f_2 + f_3 + f_4, \quad (13)$$

with (for positive dielectric anisotropy)

$$f_1 = -2e^2 \mu_n, \quad (14 a)$$

$$f_2 = \frac{1}{4}[t\mu_n^2 + (t - 2\kappa^2 sr + \kappa^2 s^2 r^2)\mu_b^2 + (t - 2\kappa^2 cr + \kappa^2 c^2 r^2)\mu_h^2 + (t - 2\kappa^2 r + \kappa^2 r^2)\mu_d^2], \quad (14 b)$$

$$f_3 = -\mu_n^3 + 3\mu_n\mu_h^2 - \frac{3}{2}\mu_n\mu_b^2 + \frac{3}{2}(3c^2 - 1)\mu_n\mu_d^2 - \frac{27}{32}\mu_b^3 + \frac{3}{64}(7c^4 - 12c^3s + 36c^3 + 20c^2s - 14c^2 - 12c + 12s + 12cs + 15)\mu_b\mu_d^2 - \frac{3}{4}\sqrt{6}(cs + c + s + 1)\mu_b\mu_h\mu_d, \quad (14 c)$$

$$f_4 = \mu_n^4 + \mu_h^4 + \frac{233}{192}\mu_b^4 + 2\mu_n^2\mu_h^2 + \frac{7}{2}\mu_n^2\mu_b^2 + \frac{9}{4}\mu_b^2\mu_h^2 + \frac{1}{2}(3c^4 - 6c^2 + 7)\mu_n^2\mu_d^2 + \frac{1}{768}(251c^8 - 312c^7 + 212c^6 + 504c^5 - 30c^4 + 504c^3 + 212c^2 - 312c + 891)\mu_d^4 + \frac{1}{8}(3c^4 + 4c^3 + 18c^2 + 4c + 19)\mu_n^2\mu_d^2 + \frac{1}{12}\sqrt{6}(3cs - 4c^2 - 3c + s - 1)\mu_b^2\mu_h\mu_d + \frac{1}{24}(-12c^4 - 27c^3 + 4c^2s + 15c^2 + 39c - 8s - 56)\mu_b^2\mu_d^2 + \frac{1}{12}\sqrt{6}c^2(-c^4 + 4c^3 + 2c^2 - 12c - 9)\mu_h\mu_d^3 + \frac{9}{8}\mu_n\mu_b^3 - \sqrt{6}(c + 1)\mu_n\mu_b\mu_h\mu_d + \frac{1}{16}(-15c^4 + 24c^3s + 8c^2s + 42c^2 - 24cs + 24c - 8s - 19)\mu_n\mu_b\mu_d^2. \quad (14 d)$$

Here, remembering that $\sigma_b + \sigma_h = \sigma_d = 1$, we have defined the quantities

$$s = \sqrt{\sigma_b}, \quad c = \sqrt{\sigma_h}, \quad (15 a)$$

with $c^2 + s^2 = 1$. Also, from equations (9) and (10),

$$r = \frac{(s\mu_b^2 + c\mu_h^2 + \mu_d^2)}{(s^2\mu_b^2 + c^2\mu_h^2 + \mu_d^2)}. \quad (15 b)$$

Equations (13)–(15) summarize the free energy functional for an H^{3D} structure with space group symmetry $P6_22$ in terms of the parameters in the order parameter $\mu_{ij}(\mathbf{x})$. Note that when $\mu_h = \mu_d = 0$, we obtain the free energy expression for the two dimensional hexagonal structure found earlier [5]. Further, when $\mu_b = \mu_h = \mu_d = 0$, equations (13) and (14) are just those characterizing a disordered or nematic (N) phase in an external field [5, 16]. Thus, in any region of the phase diagram in which either H^{2D} or N has a lower free energy than H^{3D} , the minimization of $f_{H^{3D}}$ automatically yields the two dimensional or nematic structure accordingly.

2.3. The thermodynamic phase diagram

The minimization of $f_{H^{3D}}$ was carried out numerically for different points in the (κ, t, e) phase space using gradient search methods. Both analytical and numerical computations of the gradient vector were employed and identical results were obtained. Since gradient routines give only local minima, a systematic search for the global minimum was made by initiating the procedure at different points in the parameter space.

To determine the thermodynamic phase diagram, the free energy value obtained by minimizing $f_{H^{3D}}$ was compared with those of other possible structures for arbitrary values of (κ, t, e) . In addition to the three structures, N, H^{3D} and H^{2D} , we considered the cubic structures O^2 , O^5 , O_a^8 , O_b^8 and O_c^8 , and the usual cholesteric helicoidal phase (C). As noted in §1, the applied field does not, strictly, couple to the order parameter of a cubic phase since the latter cannot have an $m = \sigma = 0$ Fourier component. Therefore, including such a coupling necessitates a lowering of the symmetry, e.g. to rhombohedral or tetragonal. There is then a non-zero μ_n Fourier amplitude which, in the weak field limit, is proportional to e^2 and the term f_1 in f (see equation (11)) is proportional to e^4 . While it is possible to take this correction into account, it has been shown [6] that it is indeed small in the field region of interest [5, 6]. We therefore use (as done previously [5]) the $e = 0$ results obtained elsewhere [11] for the free energies of the three cubic structures. As these expressions are rather long, we do not repeat them here. Given the other approximations made (e.g. the limited number of Fourier components in f and the restriction to $m = 2$ amplitudes for non-zero wavevectors) this is reasonable.

The field dependent free energy of the C phase in the weak field limit has also been given elsewhere [5]. It has the simple form

$$f_C = -e^2\mu_n + \frac{1}{4}[\mu_n^2 + (t - \kappa^2)\mu_c^2] + (\mu_n^3 - 3\mu_n\mu_c^2) + (\mu_n^2 + \mu_c^2)^2, \quad (16)$$

where μ_n and μ_c are amplitudes of the $m = \sigma = 0$ and the $m = 2, \sigma = r = 1$ Fourier components, respectively. This expression must be minimized with respect to these two amplitudes.

Portions of the thermodynamic phase diagram, obtained by minimizing and comparing the free energies of the structures noted previously, are given in figure 2; the stable structures in the (e^2, t) plane for $\kappa = 1, 1.3, 1.5$ and 1.7 are shown. We may summarize the results in the figure as follows.

(a) The cubic BP (only O^2 exists in the temperature range shown in the figure) is always unstable in a sufficiently strong external field.

(b) There is always a temperature range in which a *three dimensional hexagonal phase* appears when O^2 becomes unstable. We label this structure H_a^{3D} .

(c) For still higher field values, H_a^{3D} ceases to be stable.

(d) For $\kappa = 1$ (see figure 2(a)), the H_a^{3D} region of the phase diagram is bounded by O^2 , N, C and H^{2D} . The latter, in particular, appears for fixed t in a *higher* applied field than H_a^{3D} .

(e) For $\kappa = 1.3, 1.5$, and 1.7 , the H_a^{3D} region is bounded by *five* different structures. Here *there exists a second stable three dimensional hexagonal phase* in addition to H_a^{3D} , which is labelled H_b^{3D} in figures 2(b)–2(d). Both H^{3D} structures are characterized by the $P6_22$ space group. They differ in their phases factors, i.e.

$$H_a^{3D}: \psi_2(\sigma_b, n) = \psi_2(\sigma_d, 1) = 0, \quad (17a)$$

$$H_b^{3D}: \psi_2(\sigma_b, n) = \psi_2(\sigma_d, 1) = \pi. \quad (17b)$$

This change in the phases of the structures is similar [11] to that differentiating O_a^8 and O_b^8 from O_c^8 .

(f) The H_b^{3D} region, like H^{2D} , also appears, for fixed κ and t , in higher applied fields than H_a^{3D} with, roughly, H^{2D} lying *above* H_b^{3D} in the (e, t) phase plane.

(g) At still higher field values, all the hexagonal phases (and C) eventually become unstable and N is the only stable phase.

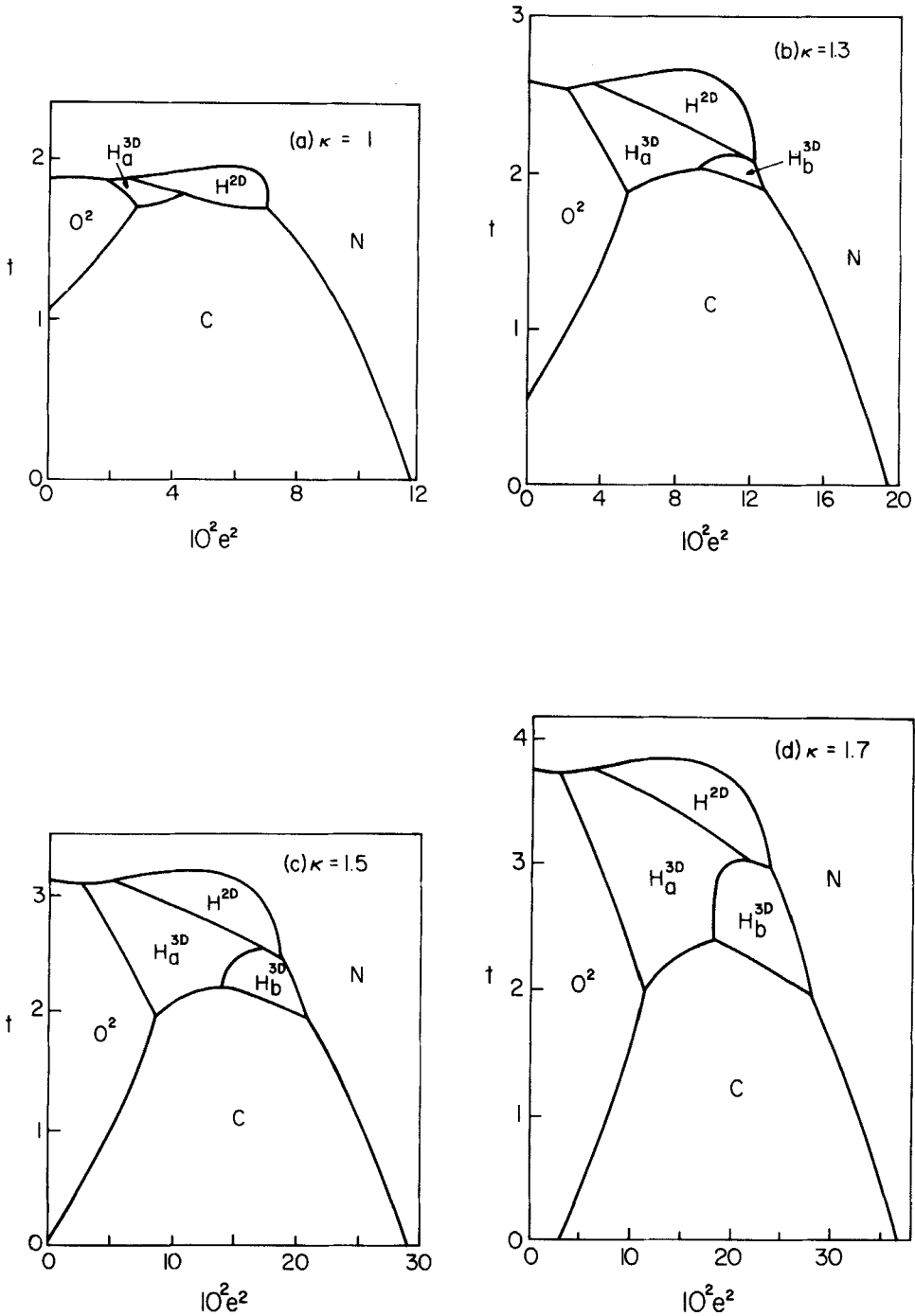


Figure 2. Cross sections of the thermodynamic phase diagram. Shown is the field (squared)-temperature (e^2 , t) plane for the following values of the chirality parameter: (a) $\kappa = 1$, (b) $\kappa = 1.3$, (c) $\kappa = 1.5$ and (d) $\kappa = 1.7$. Shown are the regions in the phase diagram occupied by the nematic phase (N), the cholesteric helicoidal phase (C), the simple cubic phase (O^2), the two dimensional hexagonal phase (H^{2D}), and two three dimensional hexagonal phases (H_a^{3D} and H_b^{3D}).

Table 2. Fourier amplitudes and unit cell parameters for the two three dimensional hexagonal structures. The point chosen is on the phase boundary separating these structures.

$\kappa = 1.3; t = 2.1; e = 0.3$	
H_a^{3D} :	$\mu_b = 0.46, \mu_h = 0.17, \mu_d = 0.15, \mu_n = 0.15, r = 1.21, c = 0.57, f = -0.041$
H_b^{3D} :	$\mu_b = 0.29, \mu_h = 0.19, \mu_d = 0.39, \mu_n = 0.17, r = 1.05, c = 0.30, f = -0.041$

Our main theoretical result is that, in an applied field, both two and three dimensional hexagonal phases can be thermodynamically stable, at least within the framework of possible structures considered here. For fixed κ and t an H^{3D} structure always occurs in a lower field than H^{2D} , in agreement with the experimental results of Piéranski, Cladis, and Barbet-Massin [7]. In addition, there is the possibility that two different H^{3D} structures can exist in different regions of the phase diagram.

The obvious method of distinguishing between these two structures would be to measure the intensities of the Bragg reflections corresponding to the amplitudes of the Fourier components. As an example we give, in table 2, the intensities characterizing H_a^{3D} and H_b^{3D} at a point ($\kappa = 1.3, t = 2.1, e = 0.3$) which is on the thermodynamical phase boundary separating these two structures. However, in practice [7, 8] the only reflection accessible experimentally was that along the hexagonal axis, which is proportional to μ_h^2 . Thus, identifying an H_a^{3D} or H_b^{3D} structure by measuring its b, h and d Bragg reflections and comparing measured intensity ratios with theoretical ones has not yet been possible. In §2.4 we consider, therefore, an alternative method for identifying the different hexagonal structures experimentally.

The signature of the transition from a three to a two dimensional hexagonal phase is the disappearance of the Bragg reflection parallel to the hexagonal axis. This is easy to observe experimentally [7]. However, detecting a transition between H_a^{3D} and H_b^{3D} (if both, in fact, exist) may be more difficult. For example, the intensity ratio $[\mu_h^2]_a / [\mu_h^2]_b$, from table 2, is 0.82. This jump of 18 per cent should be observable as a function of e . However, if the experimental amplitudes differ from the theoretical estimates by only ± 10 per cent, the peak intensity ratio could be very close to unity, making experimental confirmation of a phase transition by an intensity measurement difficult. Alternately, the *position* of this Bragg peak as a function of e could be measured. Theoretically, this wavelength is proportional to rs^2 which, from table 2, changes by approximately 15 per cent at the H_a^{3D} to H_b^{3D} transition. Even if the actual shift is considerably smaller than this estimate, it should be observable as line positions can generally be measured with a precision of 1–2 per cent.

2.4. Theoretical N.M.R. spectra

In earlier work [11, 17, 18] we pointed out that N.M.R. spectroscopy can be a convenient technique for differentiating between different cholesteric structures. Theoretical spectra for the C phase and for cubic BP [11, 17], particularly when partial ordering of domains in the latter by the magnetic field is taken into account [18], are in good agreement with experimental results [19]. Since the method used to calculate the theoretical deuterium N.M.R. spectra has been described elsewhere [17], we do not discuss it here. We note only that all theoretical spectra were calculated for the case of polycrystalline samples, with the hexagonal axes of the crystallites aligned parallel to the applied field. Perpendicular to this direction, the distribution was random.

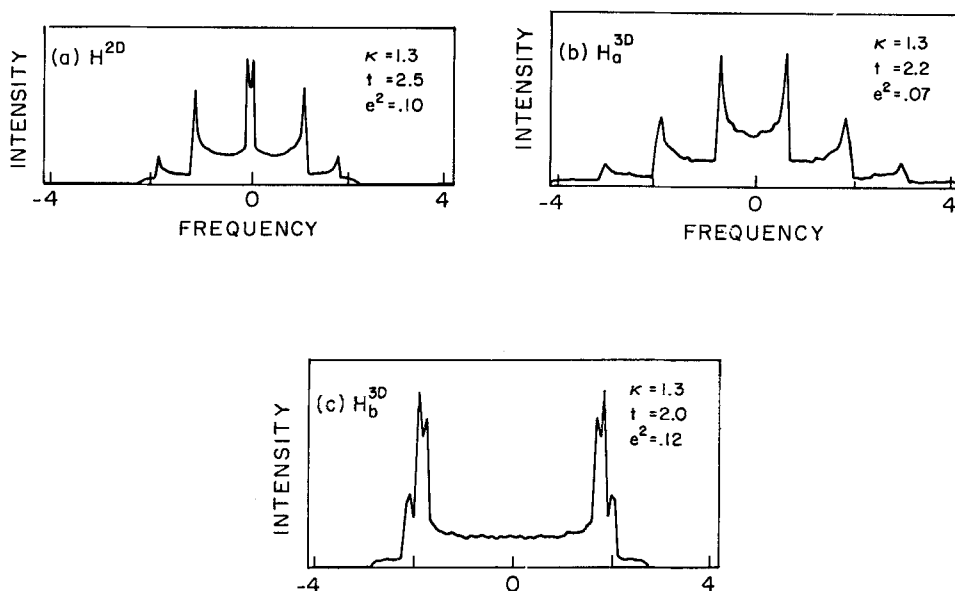


Figure 3. Theoretical deuterium N.M.R. spectra for (a) the two dimensional hexagonal structure H^{2D} and (b), (c) the three dimensional hexagonal structures H_a^{3D} and H_b^{3D} , respectively. The specimens are taken to be partially aligned such that their hexagonal axis is aligned with the applied field (which may be either magnetic or both magnetic and electric).

Since a magnetic field is always present in an N.M.R. experiment, the term 'applied field' here includes this field in addition to the electric field, if any. In the latter case both fields are aligned with the hexagonal axes of the crystallites. Typical results, for H^{2D} , H_a^{3D} and H_b^{3D} are given in figure 3. Consider first H^{2D} (see figure 3(a)). Its spectrum is quite different from those of the cubic BP and also that of the C phase [11, 17, 18]. This spectrum also differs significantly from those of the two three dimensional hexagonal structures in figures 3 (b) and 3 (c). Of the latter two, the H_b^{3D} spectrum has a pair of sharp peaks whereas for H_a^{3D} there are three well-split doublets.

Summarizing, it appears, in particular, that the differences in the deuterium N.M.R. spectra of the two possible three dimensional hexagonal structures could be sufficient to distinguish between them. Thus, this technique deserves further consideration.

3. Discussion

In this paper we have extended earlier work on the phase diagram of cholesterics in an applied field [5]. In addition to the structures considered earlier (cubic, helicoidal cholesteric, nematic and two dimensional hexagonal), we have considered the possibility that three dimensional hexagonal structures may characterize the ground state in some region of the chirality-temperature-field space. Our main result (see figure 2) is that such structures can indeed exist, in agreement with experiment [7]. Moreover, we find that *two* different three dimensional hexagonal phases may appear, both having the same space group, but differing in their structure factors. These

phases are in addition to the two dimensional hexagonal one considered earlier, which remains the stable structure in another part of the phase diagram.

Since the observed H^{3D} phase appears in a lower field than H^{2D} , it is more likely that H_a^{3D} is the structure seen experimentally. However, confirmation of this and, in particular, the observation of a second H^{3D} phase would be further evidence for the usefulness of the Landau theory approach to the cholesteric BP. Regarding H_b^{3D} , it is important to note that, theoretically, it occurs in systems with shorter pitches than those in which H_a^{3D} is predicted. Since Bragg scattering measurements, so far at least, has been limited to reflections parallel to the hexagonal axis [7, 8], we suggest that N.M.R. studies may be an additional useful approach to characterizing the hexagonal phases.

We have already noted that the theoretical phase diagram is in agreement with the experimental finding that H^{3D} appears in a lower field than H^{2D} . Lacking, however, is the observed [7, 8, 20] C phase region between H^{2D} and N. This is possibly due to our ignoring distortions (e.g. additional Fourier components) in the order parameter for the helicoidal structure. Including such terms would lower f_c and could, therefore, result in the appearance of this phase between H^{2D} and N. However, this requires further study.

The main limitation on our results is that a body-centred tetragonal phase (T^{3D}), which has been observed experimentally [7], was not considered. Extending the theoretical model to include T^{3D} is straight forward, but time consuming. Whereas it was sufficient to include only *three* non-zero wavevectors sets for H^{3D} , a realistic T^{3D} model requires *five*: basal ($n = 2$), tetragonal axis ($n = 1$), vertex-to-body centre ($n = 4$), face diagonal ($n = 4$) and base diagonal ($n = 2$) vector sets. This is necessary as the shape and size of the tetragonal cell can be such that the magnitudes of these five vector sets *all* lie between the smallest (basal) and largest (diagonal) of the H^{3D} structure. With the addition of the nematic-like component of the order parameter, we see that a minimal description of T^{3D} requires *six* order parameter components, compared with *four* for H^{3D} . This approximately increases the number of terms in f_3 and f_4 by factors of two and four, respectively. Nevertheless, given that experimental results show that T^{3D} exists, this structure must be included in order to have a complete theoretical model.

To summarize, we have shown that both two and three dimensional hexagonal structures can exist in cholesteric liquid crystals in the presence of an applied field. In particular, the results indicate that two different three dimensional hexagonal phases may exist. Some avenues for further experimental and theoretical work have been noted.

R.M.H. acknowledges the hospitality of the Liquid Crystal Institute, Kent State University, where part of this work was carried out. We are grateful to P. Piéranski and B. Jérôme for clarifying comments and to Ms Ann Sauvage for programming assistance.

References

- [1] STEGEMEYER, H., BLUMEL, TH., HILTROP, K., ONUSSEIT, H., and PORSCH, H., 1986, *Liq. Crystals*, **1**, 3.
- [2a] BELYAKOV, V. A., and DIMITRIENKO, V. E., 1965, *Usp. fiz. Nauk*, **146**, 365 (transl. 1985, *Soviet Phys. Usp.* **28**, 535).
- [2b] HORNREICH, R. M., and SHTRIKMAN, S., 1988, *Molec. Crystals liq. Crystals* (in the press).

- [3] HORNREICH, R. M., KUGLER, M., and SHTRIKMAN, S., 1988, *Phys. Rev. Lett.*, **48**, 1404.
- [4] HORNREICH, R. M., and SHTRIKMAN, S., 1986, *Phys. Rev. Lett.*, **56**, 1723; ROKHSAR, D. S., and SETHNA, J. P., 1986, *Phys. Rev. Lett.*, **56**, 1727. FILOV, V. M., 1986, *Pis'ma Zh. eksp. teor. Fiz.*, **43**, 523 (transl. 1986, *JETP Lett.*, **43**, 677).
- [5] HORNREICH, R. M., KUGLER, M., and SHTRIKMAN, S., 1985, *Phys. Rev. Lett.*, **54**, 2099; 1985, *J. Phys., Paris*, **46**, C3-47.
- [6] LUBIN, D., and HORNREICH, R. M., 1987, *Phys. Rev. A*, **36**, 849.
- [7] PIÉRANSKI, P., CLADIS, P. E., and BARBET-MASSIN, R., 1985, *J. Phys., Paris, Lett.*, **46**, L-973. CLADIS, P. E., GAREL, T., and PIÉRANSKI, P., 1986, *Phys. Rev. Lett.*, **57**, 2841. PIÉRANSKI, P., and CLADIS, P. E., 1987, *Phys. Rev. A*, **35**, 355. JORAND, M., and PIÉRANSKI, P., 1987, *J. Phys., Paris*, **48**, 1197.
- [8] PORSCH, F., and STEGEMEYER, H., 1986, *Chem. Phys. Lett.*, **125**, 319; 1987, *Liq. Crystals*, **2**, 395.
- [9] DE GENNES, P. G., 1975, *The Physics of Liquid Crystals* (Clarendon Press).
- [10] GREBEL, H., HORNREICH, R. M., and SHTRIKMAN, S., 1983, *Phys. Rev. A*, **28**, 1114; 1983, **28**, 3669(E).
- [11] GREBEL, H., HORNREICH, R. M., and SHTRIKMAN, S., 1984, *Phys. Rev. A*, **30**, 3264.
- [12] BRAZOVSKII, S. A., and DMITRIEV, S. G., 1975, *Zh. eksp. teor. Fiz.*, **69**, 979 (1976, *Soviet Phys. JETP*, **42**, 497).
- [13] HORNREICH, R. M., and SHTRIKMAN, S., 1980, *J. Phys., Paris*, **41**, 335; 1981, **42**, 367(E).
- [14] WRIGHT, D. C., and MERMIN, N. D., 1985, *Phys. Rev. A*, **31**, 3498.
- [15] HORNREICH, R. M., and SHTRIKMAN, S., 1987, *Phys. Rev. Lett.*, **59**, 68. HORNREICH, R. M., 1989, *Aperiodic Crystals*, edited by M. Jarić (Academic Press) Vol. 3, in press.
- [16] HORNREICH, R. M., 1985, *Phys. Lett.*, **109A**, 232.
- [17] GREBEL, H., HORNREICH, R. M., and SHTRIKMAN, S., 1983, *Phys. Rev. B*, **28**, 2544.
- [18] HORNREICH, R. M., and SHTRIKMAN, S., 1987, *Phys. Rev. Lett.*, **59**, 68.
- [19] SAMULSKI, E., and LUZ, Z., 1980, *J. chem. Phys.*, **73**, 142.
- [20] PIÉRANSKI, P., and JÉRÔME, B. (private communication).